The VIOCADEAS Project: Structural acoustics of good and bad violins

George Bissinger
Physics Department
East Carolina University
Greenville, NC 27858

ABSTRACT
Quality-related trends in modal and acoustic radiation measurements on 17 "bad-to-excellent" quality-rated violins in the VIOCADEAS database were explored by contrasting the properties of "excellent" and "bad" violins including three old-Italian violins *(Titian* and *Willemotte* Stradivari and *Plowden* Guarneri del Gesu, all "excellent"). This database now includes the first 3-dimensional modal analyses to investigate *extensional* as well as flexural motions, a natural consequence of curved shells. Irrespective of quality all tested violins showed the same five "signature" modes below 600 Hz (some showing coupling to the neck-fingerboard or tailpiece), with no obvious quality trends for mode frequencies or total damping. Statistical analyses of band-/modal-averaged total, radiation and internal damping, as well as directivity (ratio of top to back radiation), fraction-of-vibrational-energy-radiated, effective critical frequency, and radiativity profiles up to 4 kHz generally showed no "robust" "bad-excellent" differentiators, with one significant exception. A0, near 280 Hz, the Helmholtz-like cavity mode and the only strongly radiating resonance in the violin's lowest octave, was significantly stronger for "excellent" than "bad" violins, with "good" violins being intermediate. Radiation and total damping of two old-Italian violins appeared slightly higher than those for "bad" violins below 2 kHz, a consequence of lower effective critical frequency and slightly lower mass. Surprisingly Stradivari violins showed the highest *and* lowest directivity of all instruments tested, with a suggestive correlation to arching seen in the data. The *Titian* and *Plowden* directivity – the ratio of hemisphere-averaged radiativity from the top relative to the back - appeared correlated with their top (but not back) plate flexural/extensional mobility ratios. An interesting peak near 2.4 kHz (BH peak) was observed in the extensional - but not flexural - motion in the "bridge-island" between the *f*-holes, coinciding with a bridge/bridge-island impedance ratio minimum.

PACS no. 43.75.De, 43.40.At

NOMENCLATURE and SYMBOLS used in text

ω – angular frequency = 2π x frequency f.

Mode – a particular way an object has of vibrating at a particular frequency, with a unique motion profile. The violin has cavity, corpus (top+ribs+back), or substructure (tailpiece, bridge, or neck fingerboard) modes.

Linear system – strike an object with a certain force and it responds, strike it with twice the force and get twice the response. The response/force ratio then is constant.

Normal mode – in a linear system a unique way of vibrating that cannot be gotten by adding up any of the other normal modes.

$Y(\omega)$ – mobility = complex ratio of velocity/force (complex here means having a magnitude and a phase).

$R(\omega)$ – radiativity = complex ratio of far-field pressure/force.

$\langle R \rangle$ – over-a-sphere root-mean-square (rms) radiativity.

$\langle R_{top} \rangle$,$\langle R_{back} \rangle$ - top, back hemisphere (rms) radiativity.

$\langle D(\omega) \rangle$ - directivity, a rough measure of directionality $\langle D(\omega) \rangle = \langle R_{top}(\omega) \rangle / \langle R_{back}(\omega) \rangle$.

R_{eff} – radiation efficiency. Depends on $\langle R^2 \rangle$ and $\langle Y^2 \rangle$. Geometry-insensitive but requires radiating area. *Quantifies vibration-acoustic energy transformation.*

ζ_{tot} – total damping. Damping refers only to how a vibrating violin loses energy. Not directly sensitive to materials or geometry. Total means summed over all vibrational energy loss paths. The units are in %-of-critical (= 100/2Q).

ζ_{rad} – radiation damping – a component of total damping that requires radiation efficiency, frequency and violin mass.

ζ_{fix} – support fixture damping (≈ 0, but not for violinist holding!)

ζ_{int} – internal damping = heat losses, computed from $\zeta_{tot} - \zeta_{rad}$.

f_{crit} – critical frequency, where the flexural wave velocity catches up with the speed of sound.

$F_{RAD} = \zeta_{rad}/\zeta_{tot}$ = fraction-of-vibrational-energy-radiated.

F_f – fraction-of-radiation-from-*f*-holes.

I. INTRODUCTION

This article briefly summarizes almost 10 years of wide-ranging vibration and radiation measurements on 17 violins, and a complete violin octet, creating the VIOCADEAS database [1-10]. These measurements employed technologies initiated in the 1980s - experimental modal analysis, near-field acoustical holography, zero-mass-loading excitation-response transducers, finite element and boundary element method computational techniques along with CT scan technology (to provide shape and density information) - all of which relied on the concurrent, equally rapid development of the computer. Such technologies have provided entirely new and comprehensive ways to characterize the violin's dynamic and material properties.

The VIOCADEAS database now combines 1-dimensional (1D) calibrated modal analyses of 12 quality-rated violins (including bridge, tailpiece and neck-fingerboard substructures) and the first-ever 3-dimensional (3D) scans of 3 old-Italian and 1 modern violin [10] all with calibrated acoustical scans over a sphere in an anechoic chamber. This database was mined for possible "robust" empirical parameter-quality relationships – an elusive scientific goal for almost two centuries - using a variety of approaches based on "normal modes", a traditional physics-based way of looking at complex mechanical systems that is rooted in the profound linkage between materials and their possible ways of vibrating. It is the particulars of surface motion – a mode "shape" (often presented in terms of its nodal line structures) – that determine how the violin radiates, its structural acoustics.

With such extensive experimental information about violin vibrations including *f*-hole air motions *and* material properties with detail never previously realizable, individual normal mode behaviors can be examined, or more statistically-oriented analysis using modal or band averages. Mating these capabilities with the potential to simulate these very vibrations [7] presents an opportunity to reverse-engineer a violin back to its materials.

There are now at least fifteen structural acoustics parameters that can be used to characterize a violin or its major substructures, the top and back plate [5]. Such detailed information has led to some interesting simplifications, e.g., irrespective of quality, all traditional violins (and a complete violin octet [2,3]), properly constructed and set up, have only five "signature" normal modes in the open string region strings (196 to 660 Hz for A = 440 Hz) - albeit sometimes tailpiece or neck-fingerboard substructures can couple to these modes, splitting them into two modes, e.g., the corpus shows the same mode shape for each, but the tailpiece motions are antiphase between the two.

It is a basic tenet of vibrations that adding substructures to a structure carries their modes in some way along into the structure's overall response. Thus the violin's open string region, crucial to the sound of the violin, is also where the lowest plate modes are most important, modes 2 and 5 (tap tones) being especially important [11]. It is clear that the most important violin judgments are based on acoustical criteria, but to change the acoustics requires changing something mechanical. Above ~700 Hz when the violinist holds/plays the violin the total damping increases so much that mode overlap suggests more statistical analyses. Combining modal analysis with far-field acoustic radiativity measurements greatly expands the descriptive structural acoustics parameters to radiation efficiency, radiation damping, internal damping, fraction-of-vibrational-energy-radiated, and effective critical frequency [5].

The use of curved shells for the violin's top and back implies significant extensional motion (for example, if a curved plate is placed on a flat surface and pressed down, its flexural motion is accompanied by its edges extending outward). The intractable analytical problem of determining relative contributions of flexural vs. extensional motion for complicated shapes like the violin can be approached experimentally in a straightforward way with 3D laser vibrometry to provide a direct insight into the way the violin partitions its vibrational energy, which in turn is linked to its radiative properties. Extensional motion, which does not lead directly to acoustic radiation, when transformed into flexural motion at boundaries or discontinuities can contribute to the overall radiation. Of exceptional importance in this regard is the boundary-discontinuity concentration in the "bridge-island" between *f*-holes, where the soundpost, bass bar and the *f*-holes themselves are situated in the very region where string energy enters the corpus through the bridge feet.

II. EXPERIMENTAL

Previous technical publications covered relevant 1D experimental details for the comprehensive violin measurement-simulation program VIOCADEAS (ref. 1-10 and extensive ref. therein). All 1D vibration measurements utilized zero-mass-loading laser scans of mobility $Y(\omega)$ at >550 points over the ribs, top-back plates, bridge, neck-fingerboard and tailpiece (latter three substructures scanned from two orthogonal directions, creating 2-dimensional scans) up to 4 kHz. The measurements over various substructures - top, ribs, back – were averaged to compute a substructure-area-weighted corpus mobility $\langle Y_{corpus} \rangle$. All 1D-3D mobility and acoustic radiativity $R(\omega)$ measurements used zero-mass-loading, force-hammer impact excitation at the G-string corner of the bridge of violins suspended "free-free" from thin elastics (support fixture damping, ≤5% of total damping, was neglected in all analyses).

All violins were measured in playing condition with undamped strings at tension (A = 440 Hz) without chin or shoulder rest. Nine of the twelve 1D-scan violins (and the Curtin violin) also had top and back plate mode frequency information provided by the maker. Two of the violins had bent, not carved, plates. Finally all violins were played by the same violinist (Ara Gregorian) for quality evaluation purposes, although time constraints in the 3D experiment necessitated a more general evaluation procedure for those violins.

Far-field radiativity scans at 266 points over an r = 1.2 m sphere in an anechoic chamber were made for all 17 violins and an over-a-sphere radiativity $\langle R \rangle$ computed. A rough measure of directionality, the directivity $\langle D(\omega) \rangle$, was computed from the ratio of the top and back hemisphere radiativities $\langle R_{top} \rangle$ and $\langle R_{back} \rangle$, resp., (in-plane microphone points dropped), $\langle D(\omega) \rangle = \langle R_{top}(\omega) \rangle / \langle R_{back}(\omega) \rangle$.

The scope of VIOCADEAS was significantly broadened with the first 3D mobility scans examining *extensional* (in the plane of the surface) as well as flexural (perpendicular to the surface) motion over a broad frequency range. Over the available 2½ day measurement period the *Titian* Stradivari (1715) and *Plowden* Guarneri del Gesu (1735) had essentially complete corpus scans, plus partial scans on the *Willemotte* Stradivari (1734, back plate only) and Joseph Curtin (2006, top plate only), plus a few high-density-point scans at specific frequencies. Three separate lasers simultaneously measured the surface velocity vector along each laser's beam direction at each point; top plate exclusion zones were somewhat larger than for 1D measurements due to neck-fingerboard, bridge, or tailpiece surface shadowing. An error of omission occurred in the automated back-hemisphere radiativity scans, covering 0-4 kHz, not 0-5 kHz as in all other 3D measurements.

The three mobility vectors were isolated into orthogonal components in a chosen frame of reference [10]. Since the violin has no flat surfaces the Y direction (perpendicular to the "plane" of the violin) - the component used for comparison with previous 1D measurements on top and back

plates - was labeled out-of-plane OP, and the XZ plane labeled in-plane IP for convenience. X and Z mobilities were analyzed separately in the "bridge-island" between *f*-holes to understand extensional motion in the crucial region where string energy enters the violin.

III. RESULTS

Mobility spectra provided normal mode frequency, total damping ζ_{tot} and mode shapes to characterize each violin's vibrations, whereas radiativity spectra provided directivity as well as radiativity "profiles" useful in characterizing violin sound. Radiation efficiency R_{eff} and radiation damping ζ_{rad}, *effective* critical frequency f_{crit} and the fraction-of-vibrational-energy-radiated $F_{RAD} = \zeta_{rad}/\zeta_{tot}$ were computed from combined mobility and radiativity measurements.

At low frequencies "signature" modes were seen for all violins irrespective of quality; these mode frequencies and total damping will be examined for trends. At higher frequencies mode overlap was so pervasive and mode shapes so variable, even for our "free-free" support, that more statistical band- or modal- average analyses and trendlines - notably to estimate f_{crit} - were utilized. The narrow string-peak structures were much narrower than the corpus peaks over the entire frequency range. The 3D vibration OP-IP measurements were examined for a possible link to radiation directivity <D>.

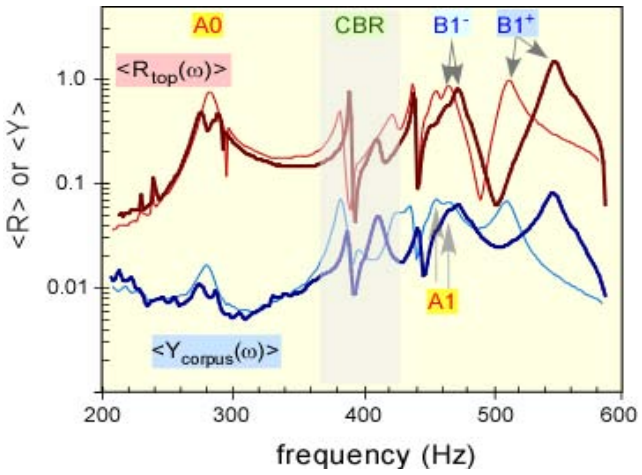

Figure 1 – Signature mode region OP (log) corpus mobility $<Y_{corpus}>$ (blue lower curves, m/s/N) and top hemisphere (log) radiativity $<R_{top}>$ (red upper curves, Pa/N) for *Titian* Stradivari (thick line) and *Plowden* Guarneri del Gesu (thin line) vs. frequency. *Titian* A0 shows neck-fingerboard or tailpiece coupling. Note low A0 mobility; narrow structures are string harmonics (always narrower than corpus peaks).

Violin subjective quality ratings were on a 1-10, three-main-class rating scale – "bad" (1-3), "good" (4-7) and "excellent" (8-10). The new data on three old Italian violins allows comparisons between "excellent" vs. "bad" (plus all-violin averages where appropriate) to magnify possible differences in quality-related parameters. Note that *quality-class* comparisons are stressed rather than individual violin results. Only "robust" quality quantifiers – where standard deviation error bars did not overlap – will be given much consideration. Even robust quantifiers however require extensive corroboration.

A. Mobility and radiativity

1. *Signature modes*

Our discussion of individual modes is limited to just the low-lying "signature" modes (the strongly radiating A0, $B1^-$ and $B1^+$ modes in the open-string, 196-660 Hz region are crucial to violin sound):

1. *Cavity modes* A0 and A1- where A0 ($f_{A0} \approx 280$ Hz) is always the lowest frequency mode characterized as a Helmholtz-like mode and always a strong radiator, while A1, the 1st longitudinal mode with frequency $f_{A1} \approx 1.7 \times f_{A0}$, is only sometimes an important radiator, but it is *coupled to A0* strongly affecting its volume dependence [12],
2. *Corpus modes* CBR, $B1^-$ and $B1^+$ - the lowest frequency corpus modes with CBR, near 400 Hz, having shear-like IP relative motion between top and back plates, a ‡ OP nodal line pattern on top and back plates, out-of-phase *f*-hole volume flows and relatively weak radiation, while the 1st corpus bending modes $B1^-$ and $B1^+$ both radiate strongly from the surface *and* through the *f*-holes [9].

Figure 1 shows the corpus OP mobility $<Y_{corpus}>$ and top hemisphere radiativity $<R_{top}>$ for the *Titian* Stradivari and *Plowden* Guarneri del Gesu in the open string region with the signature modes annotated. These radiativity and mobility curves were not exceptional in magnitudes, widths, or peak placements compared to other violins.

2. *Magnitudes*

The mobility and radiativity magnitudes of "bad", "excellent" and 14 or 17-violin averages (nominally "good" violins) presented in Figure 2 appear as 250-Hz band-averages, with two important exceptions - "A0" is an average over ±10 Hz around the A0 peak, while the 400 Hz band is averaged from 300-499 Hz to exclude A0, but include CBR and $B1^-$. Higher bands are all at 250 Hz intervals; the band centered at 625 Hz always includes $B1^+$. Thus A0, $B1^-$, and $B1^+$ dominate the lowest three radiativity bands. *Intra*-band variations shown in the figure have standard deviation (s.d.) error bars as a statistical measure of variability. Radiativity provides an objective measure of how effectively forces applied at the bridge can be turned into sound without any ear sensitivity weighting. The only robust difference between "bad" and "excellent" (old Italian) violin radiativity seen in Figure 2 occurs for A0. However, both ear sensitivity and violin directivity properties can affect what we *perceive*.

The average mobility falls off smoothly above the maximum near 2.4 kHz, which was originally attributed to the bridge "rocking". A similar peak has shown up in every part of the energy chain: bridge driving point, averaged-over-bridge, bridge feet, averaged corpus mobility, and radiativity [8]. However experiments by Jansson and co-workers [13] with solid and standard bridges clearly demonstrated that this peak did not originate in the bridge rocking, a conclusion corroborated by an experiment with widely varied rocking mode frequencies [8], a matter addressed more thoroughly in a later section on 3D measurements. Some evidence of a possible "bad-excellent" difference appeared in the corpus mobility 875-1125 and 2375 Hz bands. The radiativity profile of the "bad" violins was somewhat more peaked than the "excellent", with the A0 and high frequency ends both lower. Overall "excellent" violins had a somewhat more uniform response.

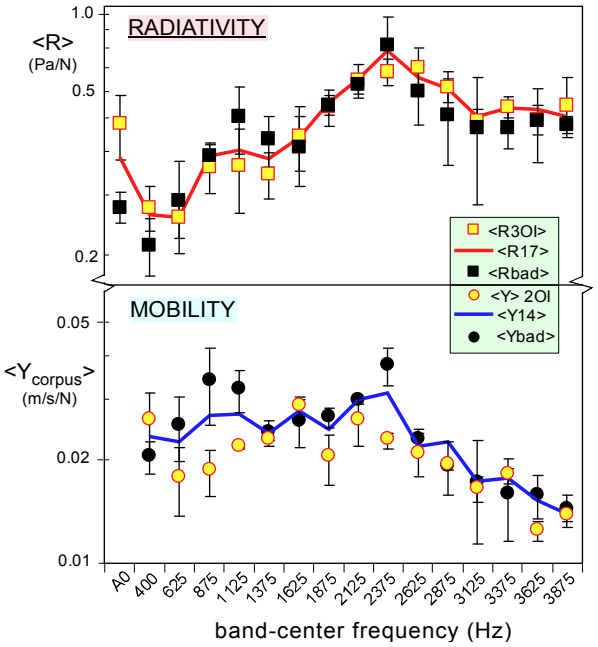

Figure 2 – (top) Band-average (log) radiativity <R> (17 violins); (bottom) band-average corpus OP (log) mobility <Y_{corpus}> (14 violins, A0 mobility omitted) vs. band-center frequency: "bad" - solid symbol, "excellent" - open symbol (all old-Italian), and average – solid line (average is nominally "good"). (s.d. error bars reflect *intra*-band variations only.)

B. **Violin mode properties vs. quality**

Violin normal mode properties were sorted by their subjective quality rating for summary purposes. The same excellent violinist Ara Gregorian played all violins; the overall ratings for 12 VIOCADEAS violins used a systematic multi-parameter rating scheme, while the Curtin, Zygmuntowicz, Stradivari and Guarneri del Gesu violins in the 3D experiment were all evaluated in a different way and have numerical ratings supplied by the author based on Gregorian's comments while playing, listeners comments and in case of the old-Italian violins their historical summary status. Such qualitative ratings should not be considered absolute in the sense of some other excellent violinist coming to exactly same numerical value but rather as a reasonably reliable evaluation based on a consistent rating scheme.

1. *Signature mode frequency and damping*

The signature modes are important because they are the only mode in the open string region crucial to violin sound. Martin Schleske, the prominent German violin maker who has been a leader in incorporating modal analyses into violin making, stated [14] that the frequency of $B1^{(+)}$ acts as a "tonal barometer" for violin sound, with frequencies <510 Hz leading to a "somewhat "soft" violin with dark sound, lacking "resistance" to bowing. On the other hand frequencies >550 Hz were characteristic of "…‚stubborn' violins with bright sound, possibly with a tendency to harshness, and with strong ‚resistance' to the player." It is unclear how a 10% change in corpus $B1^{+}$ frequency could cause such a change in perceived mechanical response since the string terminations are relatively insensitive to corpus vibrations except in the case of wolf-tones.

There is also the problem of "mechanical" characterizations being sensitive to the *sound*. Rohloff, in a experiment where filtered violin sound reached the violinist only through headphones, found that a violin's "resistance" was linked, not to the bowing force needed to initiate tones as one might expect, but rather to *acoustic strength above 4 kHz*: "easy-speaking" violins had extended response above 4 kHz, "hard-speaking" violins had limited response [15].

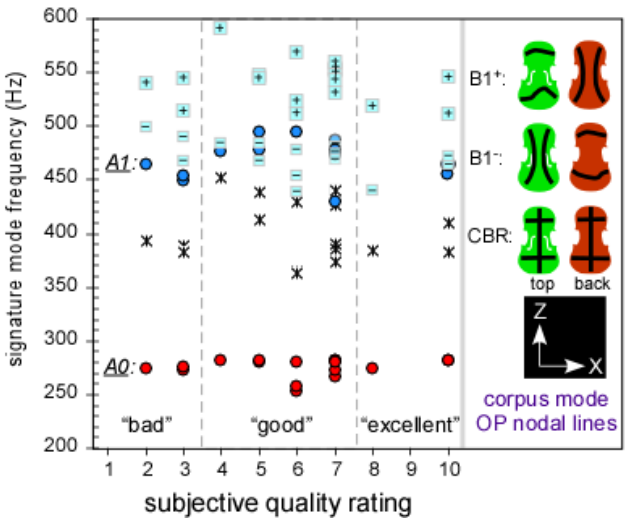

Figure 3 – Signature mode frequencies vs. subjective quality rating for 17 violins: A0 (red ●), A1 (blue ●); CBR (∗), and $B1^{-}$ and $B1^{+}$ (shaded squares with – or +). "Excellent" violins all old-Italian. Corpus mode OP nodal line patterns shown on right for reference.

Schleske's remarks suggest also that the $B1^{+}$ frequency might be a possible quality indicator. However, plotting $B1^{+}$

along with other signature mode frequencies for all 17 violins in Figure 3 vs. their subjective quality rating shows no significant correlation for any signature mode. No robust quality indicators emerged from scrutiny of signature mode total damping either. Overall A0 averaged 275 ± 9 Hz (s.d. errors: min. 253 Hz, max. 282 Hz), A1 averaged 469 ± 19 Hz (430 to 494 Hz), CBR averaged 407 ± 31 Hz (363 to 452 Hz), $B1^-$ averaged 475 ± 16 Hz (439 to 500 Hz), and $B1^+$ averaged 541 ± 22 Hz (511 to 591 Hz). The A1-A0 frequency ratio, 1.71 ± 0.05, was in close agreement with values obtained for a rigid violin-shaped cavity [12].

The two bent wood violins (6,7 ratings) were unexceptional. Considering the remarkable range of frequencies for the 6-7-rated "good" violins, the only reasonable conclusion to be drawn from Figure 3 is that signature mode frequencies or total dampings are not robust quality indicators.

2. *Damping trends*

Power-law trendlines of the form $\zeta_{tot} = Cf^{x}$ were used to quantify damping falloff trends, with $x \approx -0.5$ a value commonly seen for various structures [16]. Note that measured total damping falloff for isolated top and back plates was significantly slower than for the corpus [5], and consistent with $x \approx 0$. Clearly structural joints are affecting the total damping behavior significantly.

Damping falloff trends are shown in Figure 4 between the *Plowden-Titian* and the "bad" violin data sets. The *Plowden-Titian* trendline exponent, $x = -0.40$, was within error of the "bad" $x = -0.45 \pm 0.05$ [6]. It is clear that total damping trends are *not* robust quality discriminators. Overall, total damping trends were similar among violin quality classes. *Plowden-Titian* total damping values were always slightly larger, although within error of the "bad" violin values in any band below 4 kHz primarily due to a radiation damping difference.

The radiation damping was computed from R_{eff} ($\zeta_{rad} \propto R_{eff}/fM$, where M = violin mass, f = mode or band-center frequency). R_{eff} rises approx. as the frequency-squared until $f = f_{crit}$, then $R_{eff} = 1$ ("plateaus") above f_{crit}, creating a "knee" in the ζ_{rad} frequency dependence at f_{crit} [6], a maximum in the fraction-of-vibrational-energy-radiated $F_{RAD} = \zeta_{rad}/\zeta_{tot}$, and the most efficient region for vibration-sound conversion.

The support fixture damping ζ_{fix} was ≤5% of ζ_{tot} for our "free-free" suspension and therefore neglected. Since $\zeta_{tot} = \zeta_{rad} + \zeta_{int} + \zeta_{fix} \approx \zeta_{rad} + \zeta_{int}$ - knowing ζ_{tot} and ζ_{rad} offers the only reliable way to compute ζ_{int} for internal (heat) losses in a structure. Figure 4 shows "excellent" (*Plowden-Titian*) radiation damping higher than "bad" (although still with overlapping error bars) except for the 1375-1625 Hz bands. Lower ζ_{rad} observed for "bad" violins was consistent with higher effective critical frequencies *and* higher violin mass. ("Bad" violin masses were ~10% higher than "excellent".)

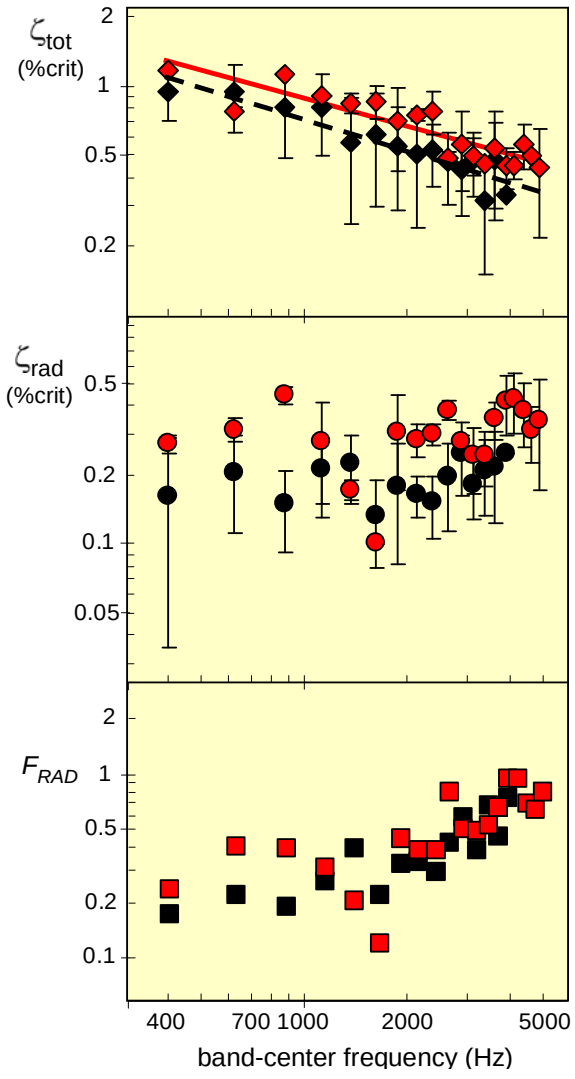

Figure 4 – Band-averaged (log) ζ_{tot} (top, with power law trend lines: red = "excellent", dashed = "bad"), (log) ζ_{rad} (middle) and (bottom) (log) F_{RAD} (= ζ_{rad}/ζ_{tot}) for "excellent" (red-filled symbol) and "bad" (black-filled symbol) violin subsets vs. (log) band-center frequency. *Intra*-band s.d. error bars (top-middle); average F_{RAD} propagated errors (not shown) nominally ±40%.

Higher "excellent" ζ_{rad} led to higher F_{RAD} values across the frequency span even though ζ_{tot} was also larger; the difference was more apparent at the lower frequencies, essentially disappearing above 2 kHz, although propagated errors were so large (±40%) that little could be made of any difference. Note that F_{RAD} - the "egress" filter for vibration-sound energy conversion - is completely independent of the "gatekeeper" filter, the violin bridge, which intermediates the initial string-corpus vibrational energy transfer. Holding the violin makes support fixture damping (now the violinist!) dominate the total damping and leads to the violinist possibly perceiving a different situation when comparing "excellent" to "bad" violins; F_{RAD} decreases as expected (~50%), but the *relative difference* between violins increases [5]. F_{RAD} peaks

near those frequencies most strongly affected by bridge rocking mode frequency changes [8], *and* where the ear is most sensitive, an interesting "coincidence".

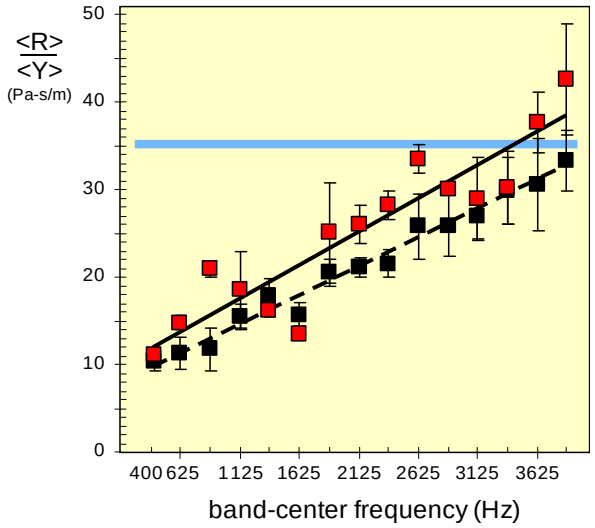

Figure 5 – Effective critical frequency estimates from 250 Hz band-averaged corpus <R>/<Y> for two "excellent" (□ - red-filled) and three "bad" violins (■) vs. band-center frequency, with linear trendlines ("excellent" solid, "bad" dashed). (s.d. error bars reflect *intra*-band variations only.) Lowest band center at 400 Hz. VIOCADEAS setup: f_{crit} (R_{eff} = 1) at <R>/<Y> = 35.2 Pa-s/m (broad blue line).

The internal damping of the violin, $\zeta_{int} \approx \zeta_{tot} - \zeta_{rad}$, falls off with frequency somewhat faster than ζ_{tot} since ζ_{rad} increases slowly up to f_{crit}. Because internal damping is similar between these extreme violin quality classes - and propagated errors so large - no definite statement is possible. Practically speaking, at f > 3 kHz, heat losses from air and surface absorption effects in a large auditorium – to say nothing of the expected violinist "support fixture" damping - are likely more important than internal damping.

3. R_{eff} and effective critical frequency

Due to its insensitivity to any shape-material properties of the vibrating object, radiation efficiency becomes a very useful structural acoustics parameter to quantify the violin's vibration-radiation conversion. R_{eff} depends on the ratio $<R^2>/<Y^2>$ for each mode with some experimental constant factors involved. This implies a frequency-squared dependence and 2nd order polynomial trendline.

While it is possible to estimate critical frequency for flat wood plates, the shape and materials make accurate critical frequency estimates impossible for a violin, and to add to the difficulty the orthotropic nature of wood gives two values! Hence *effective* critical frequencies f_{crit} were estimated initially from experimental R_{eff} trendlines solved for R_{eff} = 1 [6]. Mode-to-mode R_{eff} varied widely however. Even in successive 250-Hz bands with 2-4 modes, substantial adjacent-band jumps were common, leading in turn to occasional unreliable 2nd order polynomial fits.

This difficulty was mostly circumvented by using band-averaged <R>/<Y> plots to "linearize" the data; for the VIOCADEAS setup f_{crit} was determined by solving the trendline equation for <R>/<Y> = 35.2 Pa-s/m. Normally linear and 2nd order polynomial trendline f_{crit} values were averaged. For f_{crit} values differing by more than 5%, an exponential trendline was also fit, and added to the average.

The band-average <R>/<Y> data for "bad" and "excellent" violins in Figure 5 shows a distinct difference across the entire range, with the "excellent" linear trendline always above the "bad", crossing the 35.2 Pa-s/m line at ~3.5 kHz, while the "bad" trendline crosses near ~4.3 kHz, defining f_{crit} for each quality class. Thus the "excellent" violins were more efficient at turning vibrational energy into sound up to f_{crit}; above f_{crit} both are equally efficient. The overall average f_{crit} violin value, 3.9 kHz, was in good agreement with 4.5-4.9 kHz values computed by Cremer for violin-size flat rectangular spruce and maple wood plates (cross-grain), with along-grain f_{crit} values two octaves higher [21].

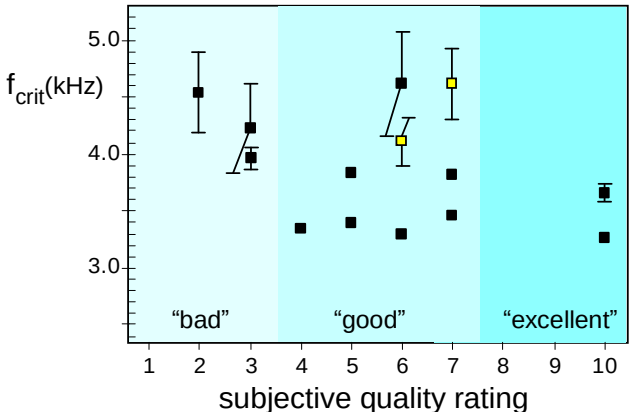

Figure 6 – f_{crit} vs. subjective quality rating for 14 violins (□ - bent wood violins, all others carved plates). (s.d. errors reflect variation between various trendline estimates only; point size hides smallest errors.)

The dip near 1625 Hz is a universal aspect of violin R_{eff} curves, suggesting a link to the "ring" frequency for cylinders, nominally 1 kHz for violins [6]. Relative prominence near this band is associated with "nasality" in the overall tone. Higher "excellent" violin ζ_{rad} in Figure 4 follows directly from increased <R>/<Y> and the resultant lower f_{crit}, in combination with lower mass. A plot of f_{crit} vs. quality rating for 14 violins presented in Figure 6 might make a case for a significant difference between "bad" and "excellent", but the best of the "good" violins shows a range encompassing these quality extremes, undermining any robust quality-related trend. Also machine-figured plates in factory violins typically run significantly thicker than these tested "bad" violins, implying a lowered critical frequency.

4. *Directivity*

Although Figure 2 showed little difference in averaged-over-sphere radiativity between "bad" and "excellent" violins, the violinist would be expected to hold the violin in the way that most effectively gets the sound to the audience, implying that violin sound directionality is an important facet of being heard over the orchestra. Our directivity, a simple measure of sound directionality, shows the top radiates more effectively than the back. The sound from the back also effectively has two extra (floor-back wall) bounces before heading into the hall, further diminishing its importance. The directivity <D> = $<R_{top}>/<R_{back}>$ is summarized for all 17 violins in Figure 7. "Bad" violin <D> generally was above the 17-violin average; the *Titian* had the highest <D> overall of any violin tested to date (with one "bad" violin quite close) and the *Willemotte* the lowest, while the *Plowden* was very close to average. Obviously directivity varies widely, even among the violins of one maker, with no link to perceived quality.

In the 625-875 Hz region where wavelength $\lambda \geq$ violin size, <D> ≈ 1 (isotropic) radiation would be expected. Surprisingly, Figure 7 highlights an unexpected behavior, viz., the fast rise of the directivity at 625-875 Hz (followed by a plateau from 1-2.5 kHz, then a slow rise above 2.7 kHz). A reasonable interpretation of this rapid rise, based on recent "patch" NAH results for just *f*-hole radiation [9] compared to the anechoic chamber measurements of corpus+*f*-hole radiation, is based on the fact that *f*-hole-only radiation contributed ~50% to the overall violin radiation at f < 1 kHz (falling off with increasing frequency) *and* was significantly more directional at lower frequencies (see dashed line, Figure 7) than expected, e.g., if the 625 or 875 Hz bands had a 50:50 *f*-hole:corpus radiation balance, then the amalgamated <D> would be (1.3+1)/2 ≈ 1.2, or (1.8+1)/2 ≈ 1.4, resp., close to 17-violin values.

5. *Arching and directivity*

Does arching affect directivity? The *Willemotte* top plate arching of 17.6 mm was highest of all violins tested (along with the Curtin violin), while the *Plowden* was the next-to-lowest at 14.1 mm. CT scan bridge slices were used to estimate arch heights ±0.3 mm; Curtin and Zygmuntowicz violins had directly measured values. Arching groups of 14-15 mm (7 violins), 15-16 mm (3 violins), 16-17 mm (5 violins) and 17-18 mm (2 violins) were plotted vs. average <D> in the 625-875 Hz and 3125-3875 Hz bands to create the inset in Figure 7.

Overall the highest arch violins appear to have lower overall directivity, with the suggestion of a maximum in the 15-16 mm range. However it is difficult to be certain that directivity is affected by arching since there might be significant effects from OP-IP ratio differences, which also imply a directivity link. This aspect of directivity is explored next in the 3D results section.

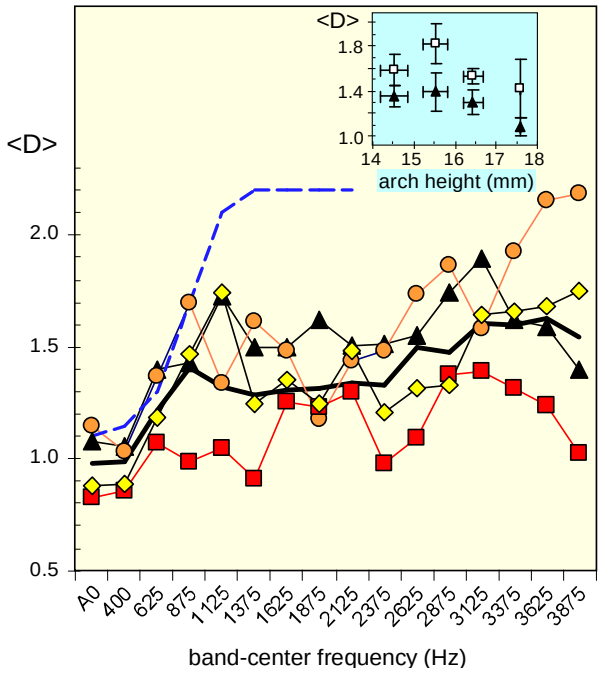

Figure 7 – Directivity for "bad" (▲), *Titian* (○-orange fill), *Plowden* (◇-yellow fill), *Willemotte* (□-red fill) and 17-violin average (thick line) vs. band-center frequency. Directivity of ***f*-hole radiation only** shown as dashed blue line. *Titian* had highest <D>, *Willemotte* had the lowest. Nominal intra-band variations 15%. (Inset: average <D> for 625-875 Hz (▲) and 3125-3875 Hz (□) regions vs. arch height for 17 violins; s. d. error bars.)

C. 3-dimensional modal analyses

Since only the flexural motions produce sound, why pay any attention to the extensional motions, a difficult and hence neglected area of violin vibratory behavior? The short answer is that there must be some extensional motion as the curved plates vibrate *and* it is possible to transform extensional into flexural motion (and *vice versa*) - at edges (e.g., rib joints) and discontinuities (e.g., bass bar, *f*-holes, soundpost). This fundamental coupling between flexural and extensional motion create an extraordinarily difficult analytic problem for complicated structures like the violin.

Experimentally however determining the relative importance of flexural vs. extensional motion is now relatively straightforward with the advent of scanning laser 3D modal analyses. These measurements allow us to investigate two important aspects of violin sound: 1) how OP-IP vibrational energy partitioning might affect violin radiation, and 2) how violin corpus motion immediately in the vicinity of the bridge feet relates to string energy transfer through the bridge feet to the corpus.

1. *OP-IP vibrations and directivity*

OP mobility in the signature mode region extracted from 3D scans was shown in Figure 1 for the *Titian* and *Plowden*. The old-Italian mobility and radiativity magnitudes were

similar to those of other violins. Of more interest here is the strength of OP relative to IP motions. The reasoning here – assuming nominally the same averaged overall magnitude – is that larger OP/IP ratios should correlate with more sound production, since only the OP component is responsible for radiation. Figure 8 presents OP/IP ratios for the top plate and back plates of all violins with 3D scans, even partial ones. Three maple backs all had similar OP/IP ratios, implying a constant radiative contribution, but the top plate OP/IP – with varied-geometry bass bars and *f*-holes - differed significantly among the violins. (Violinmaking lore has long stressed the relative importance of the top vs. back to violin sound.)

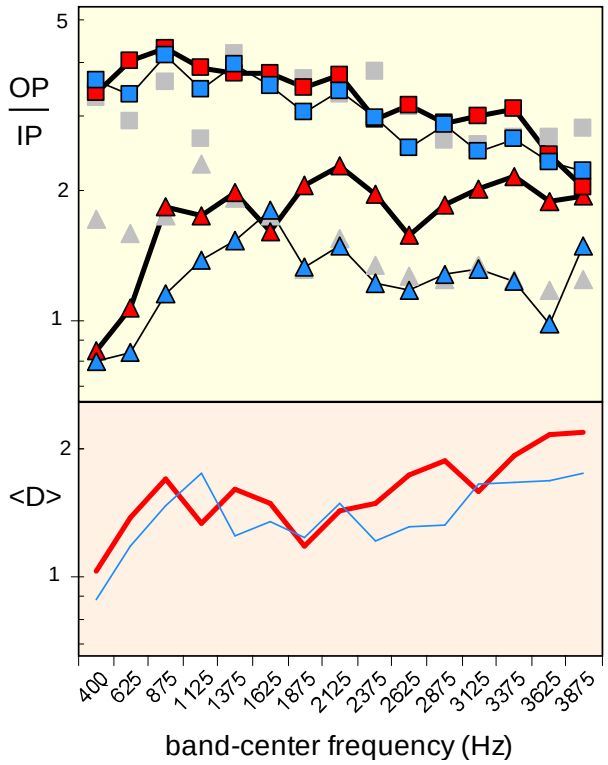

Figure 8 – Top: OP/IP (log) ratio vs. band-center frequency: **top plate** - Δ (*Titian*-red-filled, thick line; *Plowden*-blue-filled, thin line; Curtin-gray); **back plate** - ☐ (*Titian*-red-filled, thick line); *Plowden* blue-filled, thin line; *Willemotte*-gray). Bottom: (log) directivity: *Titian* (red line), *Plowden* (blue line).

Maple backs are seen to have much higher OP/IP ratios than spruce tops, and the *Titian* top plate had a much higher ratio than either the *Plowden* or Curtin violins. The measured directivity is also included in Figure 8 for the *Titian* and *Plowden*. The higher OP/IP ratio for the *Titian* was accompanied by higher directivity compared to the *Plowden*; the Curtin violin directivity was similar to the *Plowden* (both near average) and consistent with its top OP/IP ratio, and the assumption of a relatively constant ratio for the back. Some kind of arching-directivity correlation, if it is indeed real, offers a possible link to the OP/IP ratio depending on arching also. Of course the flat plate (arch = zero) has only OP motion to 1st order, and thus a very high OP/IP ratio. The practical durability reasons for non-zero arching of course are more compelling than the accompanying lower OP-IP ratios.

2. *OP-IP, BH and the "bridge-island"*

The origin of the BH peak near 2.4 kHz in OP mobility *and* its accompanying radiativity profile seen in Figure 2 is a poorly understood aspect of violin vibrations. If bridge rocking about the waist motions do not produce the BH peak what does? Durup and Jansson, in a systematic "violin" experiment using a simplified geometry violin (flat rectangular plates), observed a BH peak only *after* cutting simplified *f*-holes (3-segment, squared-off, elongated "S" shapes) into the top plate. Crucially, only the long straight section led to the BH peak *and* no BH peak appeared when this section was above the bridge [13]. If cutting *f*-holes is essential to creating the BH peak - simultaneously reducing X-direction stiffness in the bridge "island" around the bridge feet *and* creating close by boundaries-discontinuities – perhaps an alternative IP bridge→corpus→radiation path via extensional→ flexural transformation offers a plausible augmenting mechanism for OP motion, thereby leading to substantial radiation.

Actually this BH "structure" seems unusual only because of its magnitude, with typical radiation efficiency and total damping values for its frequency region. Bridge top rocking about the waist, leading to up-down antiphase bridge feet motions that excite corpus OP motion, has been proposed lately as a physical mechanism for this peak [18,19]. Even though a significant peak in OP motion was observed in $\langle Y_{corpus} \rangle$, little such antiphase motion was seen at the bridge feet near 2.4 kHz.

The sensitivity of the BH peak to changes in the bridge rocking mode frequency f_{rock}, especially at f_{rock} values closest to 2.4 kHz, where its amplitude and centroid frequency slumped noticeably (cf. fig. 10, ref. 8) does link the BH peak to the bridge motion. Because string energy enters the corpus through a tuned substructure whose optimized coupling to the corpus is essential to good violin sound [8] *and* nearby boundaries-discontinuities are abundant, especially so in the X-direction, the possibility of extensional→ flexural transformations leading to acoustic radiation makes understanding this region crucial.

Our attention is now concentrated on the 3D mobilities averaged over 19 points in a small region of the top plate near the bridge feet - the "bridge-island" (shown as an inset in Figure 9 with X and Z axes noted). The island X-Y-Z mobility components (notated as $\langle Y_X \rangle$, $\langle Y_Y \rangle$, $\langle Y_Z \rangle$) for the *Plowden*, *Titian* and Curtin violins were band-averaged separately, rather than having the X and Z components conglomerated into an IP motion as before.

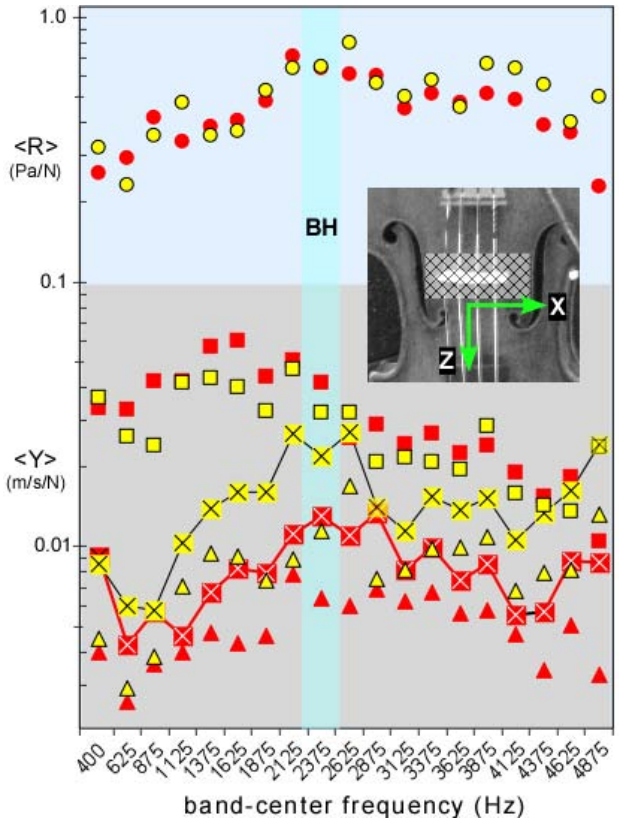

Figure 9 – *Plowden* and *Titian* comparisons: (top) (log) radiativity <R> - ○); (bottom) 3-dimensional bridge-island (log) mobility vs. band-center frequency comparison: $\langle Y_Y \rangle$ - □, $\langle Y_X \rangle$ - ☒ with lines, $\langle Y_Z \rangle$ -△. (Yellow-fill points are *Plowden*, red-fill are *Titian*.) BH region highlighted. (Inset: bridge-island region shown cross-hatched, superimposed on violin photo.)

The bridge-island 3D mobility behaviors for the *Plowden* and *Titian* are shown in Figure 9 (Curtin violin not included to reduce point clutter). The *3-violin-average* bridge-island 3D mobility behaviors present some interesting differences from the 14-violin corpus OP mobility (OP = $\langle Y_Y \rangle$) results in Figure 2:

- The $\langle Y_Y \rangle$ peak is now near 1.4 kHz, not 2.5 kHz as seen in Figure 2, with a relatively smooth falloff above this,
- $\langle Y_Z \rangle$ is overall the lowest across the range, while $\langle Y_Y \rangle$ is the highest, likely reflecting relative stiffnesses along each direction,
- $\langle Y_X \rangle$ has a definite, broad peak near 2.5 kHz, and was the only mobility component to show a definite peak in the BH region,
- $\langle Y_X \rangle$ for the *Plowden* was close in magnitude (~70%) to $\langle Y_Y \rangle$ near 2.4 kHz, with the *Titian* being much lower (~30%),
- From 625 to 4875 Hz the *Titian* $\langle Y_Y \rangle / \langle Y_X \rangle$ ratio was about twice the *Plowden* and Curtin values. It is quite possible this difference reflects the OP/IP corpus ratio and directivity results presented in Figure 8.
- The Curtin violin results were quite similar to those of the *Plowden*, with comparable $\langle Y_Y \rangle$ (and $\langle Y_X \rangle$) magnitudes and trends. The $\langle Y_X \rangle$ peak was broader than for either old-Italian; $\langle Y_Z \rangle$ was too weak-noisy for reliable analysis.

The presence of the bridge-island $\langle Y_X \rangle$ peak near 2.5 kHz for the 3-violin average suggests significant X-plane motion accompanying bridge rocking motion in string-corpus energy transfer. Unfortunately there were no bridge 3D measurements. Accordingly the 12-violin 1D bridge measurements were reanalyzed to look at X and Y bridge motions separately, and then used in conjunction with 3D bridge-island results to compute a bridge/bridge-island impedance ratio.

The bridge 1D rms mobility results had previously shown a prominent BH peak when averaged over X and Y mobilities [8]; reanalysis of X (side-only) and Y (top-only) measurements (see Figure 10 inset for point locations-directions) showed ~2.4 kHz peaks in rms mobility for both directions separately. Since string→bridge→bridge-island energy transfer is so important, a rough measure of direction-specific impedance relationships based on mobility average inverses was used to compute the X and Y impedance ratios, Z_{bridge}/Z_{island}, separately. These ratios, presented in Figure 10, show a distinct local minimum in the BH region for X and Y directions, as well as a prominent maximum near 1.3 kHz for the Y-direction. The trends seen in Figures 9 and 10 are certainly suggestive of some bridge to bridge-island excitation mechanism based on X-motion.

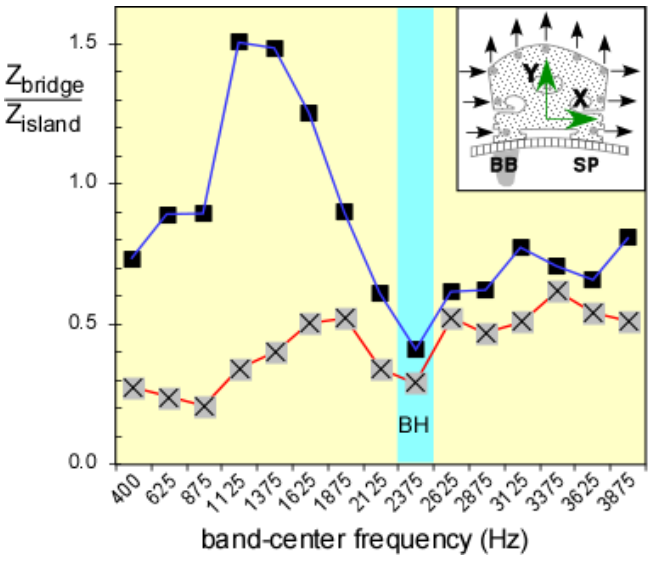

Figure 10 – Impedance ratio of bridge (1D) to bridge-island (3D) vs. band-center frequency for Y(■) and X(☒) directions. (Inset: bridge point measurement location-direction).

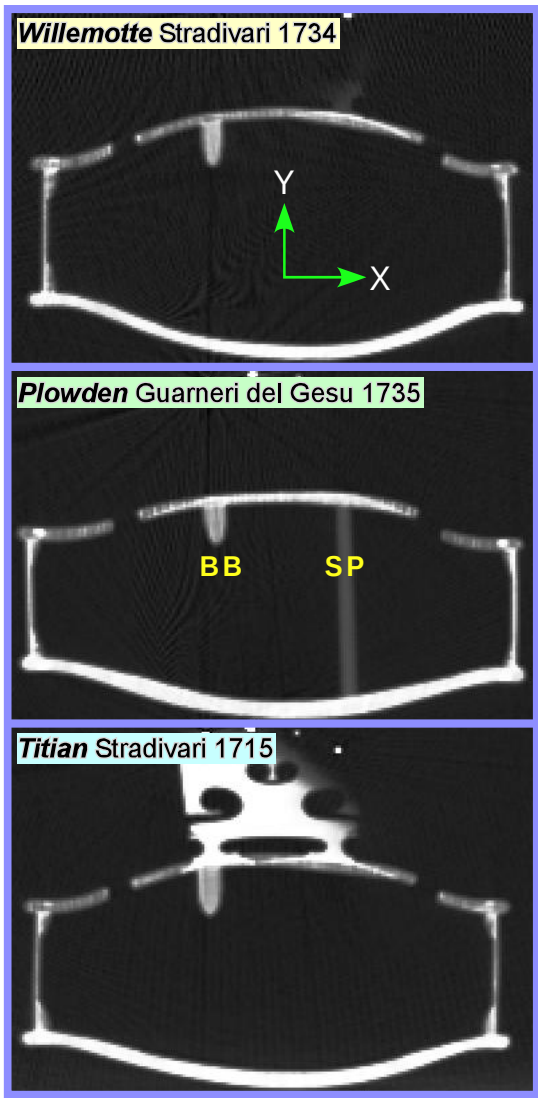

Figure 11 – CT scan slice in the bridge-soundpost region of three old-Italian violins. Repairs under bridge feet in spruce top ($\rho \approx 0.4$ gr/cm^3) over bass bar and soundpost are readily seen as higher-density (brighter) regions. (Maple back and bridge have $\rho \approx 0.6$ gr/cm^3.)

One additional, possibly pertinent note related to the old-Italian CT scans was that all these violins showed some significant internal repair work around the bridge region where the soundpost and bridge feet and bass bar replacement tend over time to disrupt the structural integrity of the soft spruce top plate (Figure 11). Localized repairs in this critical energy transfer region are a natural companion to age and playing, and are universal to instruments of the classical period. These repairs commonly require gluing in wood patches. If the patch density matched the original, and the fit were flawless only the (brighter) higher density glue-line arc would stand out in a CT scan. Standing out among these violins, the *Titian* also showed an additional, small high density patch underneath the bass bar-side bridge foot, as well as a prominent patch glue-line under the soundpost-side bridge foot. Whatever the cause of the *Titian*'s high OP-IP ratio, these repairs are mentioned because of extensional→ flexural transformations possible at discontinuities. Perhaps density discontinuities at a patch glue-line could be one such cause?

IV. CONCLUSIONS

The very best violins *measure* little different from the worst (assuming all had been properly setup of course), confirming the conclusion reached by previous researchers. All violins were observed to have similar underlying structural acoustic behavior. What was observed were different spectral balances as the relative magnitudes of various psycho-acoustically important regions changed over the profiles, perhaps tilting toward the low or high ends of the profile, or emphasizing a specific region. These shifts/emphases are important to the player as Schleske has noted [20].)

Common remarks about the best violins - they are more "even" across the measured range, and strong in the lowest range – are reflected in the "excellent" violin radiativity profiles. Loudness is also important. Typical reverberation in a large auditorium provides a low frequency boost and a high frequency rolloff above 5 kHz. Concentrating sound near 2-4 kHz, where the ear is most sensitive, and where typical orchestral sound is less prominent, the combination of BH+bridge+F_{RAD} provides a significant higher frequency "boost". The enhanced directivity seen for the *Titian* (but not the *Plowden* or *Willemotte*) could certainly help a solo violin being heard over the orchestra.

Can our experimental modal-acoustic results address such matters as pre-treating wood with various chemicals, or deal with the varnish per se? Succinctly, no. Assuming constant shape, violin response to some driving force is determined by the overall stiffness-density properties of its various materials, irrespective of how these were arrived at.

At this time the most productive area scientifically appears to be the radiativity profile, the "measurable" at the end of the energy trail that seems most immediate to a violinist in the overall judgment of violin sound quality. These radiativity profiles overall have quite similar gross characteristics, thus providing a rationale to investigate the underlying structural acoustics basis of the entire profile.

Finally some remarks about the qualitative evaluations are in order. What truly defines violin excellence? If the answer is truly excellent violinists, then the reliability-reproducibility of their psycho-acoustic judgments must draw more attention. It would seem illogical to expect violinists who pride themselves on their personal sound not to prefer certain violins over others because they are better at creating that sound. If excellent violinists cannot agree on a quality rating because of sound preferences – or worse, rate two quite different sounding violins as "good" - shouldn't it follow that scientific measurements could do no better?

ACKNOWLEDGMENTS

The 3D measurements resulted from a cooperative effort among Polytec, Inc. who provided their advanced 3D laser system (operated by David Oliver and Vikrant Palant), the East Carolina University Acoustics Laboratory (acoustics scans, author and Danial Rowe), renowned violin maker Samuel Zygmuntowicz who arranged for the loan of the old Italian violins, the Violin Society of America (Joseph Regh and Fan-Chia Tao) which paid for the insurance and transportation of the violins, and Dr. Claudio Sibata at the CT scanner in the Leo Jenkins Cancer Center at East Carolina University. In addition Samuel Zygmuntowicz and another renowned violin maker Joseph Curtin kept all instruments in optimum condition. All measurements used comprehensive test facilities constructed at East Carolina University between 1998-2003 with the aid of a National Science Foundation grant (DMR-9802656).

REFERENCES

1. G. Bissinger and A. Gregorian, "Relating normal mode properties of violins to overall quality: signature modes", Catgut Acoust. Soc. J., vol. **4**, No. 8 (Series II), 37-45 (2003).
2. G. Bissinger, “Wall compliance and violin cavity modes”, J. Acoust. Soc. Am. **113**, 1718-1723(2003).
3. G. Bissinger, “Modal analysis of a violin octet”, J. Acoust. Soc. Am.**113**, 2105-2113 (2003).
4. G. Bissinger and J. C. Keiffer, "Radiation damping, efficiency, and directivity for violin normal modes below 4 kHz", Acoust. Res. Lett. Online **4**, 7-12 (2003). http://ojps.aip.org/ARLO.
5. G. Bissinger, “Contemporary generalized normal mode violin acoustics”, Acustica **90**, 590-599 (2004).
6. G. Bissinger, “The role of radiation damping in violin sound”, Acoust. Res. Lett. Online **5**, 82-87 (2004). http://ojps.aip.org/ARLO.
7. G. Bissinger, “A unified materials-normal mode approach to violin acoustics”, Acustica **91**, 214-228 (2005).
8. G. Bissinger, “The violin bridge as filter”, J. Acoust. Soc. Am. **120**, 482-491 (2006).
9. G. Bissinger, E.G. Williams and N. Valdivia, “Violin *f*-hole contribution to far-field radiation via patch near-field acoustical holography”, J. Acoust. Soc. Am. 121, 3899–3906 (2007).
10. D.E. Oliver, V. Palan, G. Bissinger and D. Rowe, “3-Dimensional Laser Doppler Vibration Analysis of a Stradivarius Violin”, Proc. 25th Intern. Modal Analysis Conf., Soc. Exp. Mechanics, Bethel, CT, 2007, paper #372 (CD proceedings only)
11. G. Bissinger, “Surprising regularity between plate modes 2 and 5 and the B1 corpus modes: Part I”, J. Violin Soc. Am.:VSA Papers, **21**(no.1),85-103 (2007).
12. G. Bissinger, "A0 and A1 coupling, arching, rib height, and *f*-hole geometry dependence in the 2-degree-of-freedom network model of violin cavity modes," J. Acoust. Soc. Am. **104**, 3608-3615 (1998).
13. F. Durup and E. Jansson, “The quest of the violin bridge-hill”, Acustica **91**, 206-213 (2005).
14. M. Schleske, “Empirical tools in contemporary violin making: Part 1. Analysis of design, materials, varnish and normal modes”, Catgut Acoust. Soc. J., vol **4**, no.5 (series II), 50-65 (2002).
15. E. Rohloff, “Ansprache der Geigenklänge (The speaking of violin sounds)”, Z. Angew. Physik **17**,62-63(1934). English abstract published in *Musical Acoustics, Part II, Violin Family Functions*, Vol 6. Benchmark Papers in Acoustics. C.M. Hutchins, ed., Dowden, Hutchinson & Ross, Stroudsburg, PA (1976).
16. F. Fahy and P. Gardonio, *Sound and Structural Vibration: Radiation, Transmission and Response*, 2nd ed. (Academic Press, 2007, New York)
17. L. Cremer, *The Physics of the V iolin*, (MIT Press, Cambridge, 1984).
18. I.P. Beldie, “”About the bridge hill mystery”, Catgut Acoust. Soc. J. vol **4**, no.8 (Series II), 9-13 (2003).
19. J. Woodhouse, “On the bridge-hill of the violin”, Acustica **91,** 155-165 (2005).
20. M. Schleske website, http://www.geigenforschung.de/ 11handbuch/en_extras3handbuch04klangfarbe.pdf.